PERGAMON

International Journal of Solids and Structures 37 (2000) 1501–1519

INTERNATIONAL JOURNAL OF SOLIDS and STRUCTURES

www.elsevier.com/locate/ijsolstr

Dynamics of delaminated beams

H. Luo*, S. Hanagud

School of Aerospace Engineering, Georgia Institute of Technology, Atlanta, GA 30332, USA

Received 26 August 1998; in revised form 4 November 1998

Abstract

In this paper, we present a new model for composite beams with through-width delaminations. Shear effect and rotary inertia terms, as well as bending-extension coupling, are taken into account in the governing equations of vibration. Nonlinear interaction, due piecewise linear spring models between the delaminated sublaminates, is also included. Based on this model, eigensolutions for vibrations of intact and delaminated beams are found analytically. Dynamic behavior predicted by this model is then compared with previously reported experimental results. Better agreements with the experimental results are found. Discrepancies among previously proposed models are explained without difficulty. © 1999 Elsevier Science Ltd. All rights reserved.

Keywords: Delamination; Delamination modeling; Nonlinear dynamic response; Composite beam; Frequency; Mode shape; Eigensolutions

1. Introduction

Advanced composite materials are increasingly used in structural designs of aircraft, helicopters, and spacecraft because of desirable properties like high strength and stiffness, lightweight, fatigue resistance, and damage tolerance, etc. (Anon, 1992). However, composites are very sensitive to the anomalies induced during their fabrication or service life. Delaminations are found to be one of the important failure modes in composite structures (Garg, 1988). The presence of delaminations in a composite structure affects its integrity as well as its mechanical properties such as stiffness and strength. Reflections of these effects in dynamic response are the alteration of natural frequencies and damping ratios. In addition 'delamination modes' which are related to the opening of the delaminated region during the dynamic response will appear in some cases. As a result, considerable analytical, numerical, and experimental efforts have been expended to capture these phenomena.

One of the earliest models for vibration analysis of composite beams with delaminations was

* Corresponding author. Currently working for Corporate Research and Development Center, General Electric Company, Schenectady, New York, USA.

PII: S0020-7683(98)00325-4

proposed by Ramkumar et al. (1979). They modeled a beam with one through-width delamination by simply using four Timoshenko beams connected at delamination edges. Natural frequencies and mode shapes were solved by a boundary eigenvalue problem. By using their model, the predicted natural frequencies were consistently lower than the results reported in experimental measurements. Authors attributed this discrepancy to the effect of contact between the delaminated 'free' surfaces during vibrations. They suggested that the inclusion of the contact effect may improve the analytical prediction. Instead of using this suggestion, Wang et al. (1982) improved the analytical solution by including the coupling between flexural and axial vibrations of the delaminated sublaminates. Using an isotropic beam with splits and the classical beam model, they found that the calculated natural frequencies were closer to experimental results. With similar considerations, Nagesh and Hanagud (1990) formulated a finite element solution for arbitrary composite beams. In the finite element models, they considered the classical beam model as well as the beam model with high-order shear deformations. Later, Mujumdar and Suryanarayan (1988) pointed out that some delamination opening mode shapes predicted by Wang et al. (1982) are physically incompatible. They argued delamination opening modes are mathematically admissible. However, they believed that the appearance of these modes in a dynamic response is not feasible because of possible overlap between the delaminated sublaminates. To avoid this kind of incompatibility and keep a linear model, they imposed a pressure between the delaminated parts, that is, two delaminated parts were constrained to have the same flexural deformations. This model was called 'constrained model' in contrast with the 'free model' proposed by Wang et al. (1982). The 'constrained model' assumptions were also used to model simply-supported composite beams (Tracy and Pardoen, 1989) and sandwich beams (Hwu and Hu, 1993). Nevertheless, the constrained model fails to explain the delamination opening modes found in experiments (Shen and Grady, 1992). In these experiments conducted by Shen and Grady (1992), opening modes were even found in the first bending mode of the beam for some delamination cases. However, their finite element formulations (Model A and B) were essentially followed the 'constrained model' by Mujumdar and Suryanarayan (1988) and the 'free model' by Wang et al. (1982). The discrepancy between the results predicted by the two models is significant even in cases where mode shapes do not show any opening in the delamination region. Furthermore, in some cases, opening delamination modes were shown clearly in their experiment, while the 'constrained model' frequency prediction had a better match with the corresponding experimental results for these modes, even though the delamination cannot open using the 'constrained model'. In the experimental research done by Hanagud and Luo (1994), Luo and Hanagud (1995), they have indicated that the delamination modes can also be found in combination with higher order modes for structures with through-width as well as embedded delaminations.

Research on vibrations of a delaminated beam with respect to its buckled state is attributed to Yin and Jane (1992). They analyzed the vibrations of a clamped–clamped beam with a symmetrically located delamination and with buckling due to an axial force. The relative amplitude of the vibrations between sublaminates in the delamination region was assumed to be smaller than the opening under a buckling state. Thus, there can exist free delamination vibrations without impact between the delaminated sublaminates. In Chen's paper (Chen, 1994), he included shear deformation term in his postbuckled model, while in the prebuckled case, a constrained model was used, i.e., assuming the upper and lower delamination parts have the same flexural deformations.

To the author's best knowledge, we do not have an analytical model that can consistently explain the phenomena observed by experiments. The purpose of this paper is to developed a model which is able to capture the experimental phenomena without introducing contradictions. In this research, we used a piecewise-linear spring model to simulate the behavior between delaminated surfaces. Shear and rotary inertia effects, as well as bending-extension coupling, are included in the governing equations. Frequencies and mode shapes are solved through a boundary eigenvalue problem. The proposed model includes the 'free model' and the 'constrained model' as special cases. In a case where delamination

opening does not appear in the mode shape, both 'free model' and 'constrained model' cases converge to predict the same frequency. The nonlinear response simulated by this model shows good agreement with the experiment results.

2. Analytical modeling

2.1. Basic assumptions

As shown in Fig. 1, after delamination, a representative composite beam with width b, height H, and length L can be viewed as a combination of four beams connected at the delamination boundaries $x = L_1$ and $x = L_2$. In Fig. 1, we denote m_i, D_i, S_i and $A_i (i = 1, 2, 3, 4)$ the mass density per unit length, bending stiffness, cross sectional shear stiffness, and extensional stiffness of four beams, respectively. The notations H_2 and H_3 represent the distances between the neutral axis of the delaminated beam and the neutral axis of the intact part. It is worth noting that, for composite materials, $H_2 + H_3$ is not necessarily equal to $H/2$. The geometric center and the neutral axis of a sublaminate, in general, do not coincide.

The effects between the delaminated surfaces depend on the relative position between the sublaminates during vibrations. Delaminations in a composite structure usually occur in the matrix between fiber plies. Here we assume that after delamination, partially intact matrix and fibers still fill the delamination crack. Some constraints between the upper and lower delamination still exist. Under a small amplitude vibration of the delaminated beam at a frequency corresponding to a delamination opening mode, the effect between delaminated sublaminates can be modeled as a distributed soft spring between them. When the amplitude exceeds a certain level, the spring effect becomes zero because the delamination opens beyond the small amplitude constraints. On the other hand, when the vibration mode does not tend to open the delamination, the delaminated sublaminates have the same flexural displacements and slopes. Thus, the exact behavior of the effects between the delaminated sublaminates may be described by a nonlinear spring model as shown qualitatively in Fig. 2 by a dashed line.

To simplify the problem while keeping the significant nonlinear features of the vibrations of a

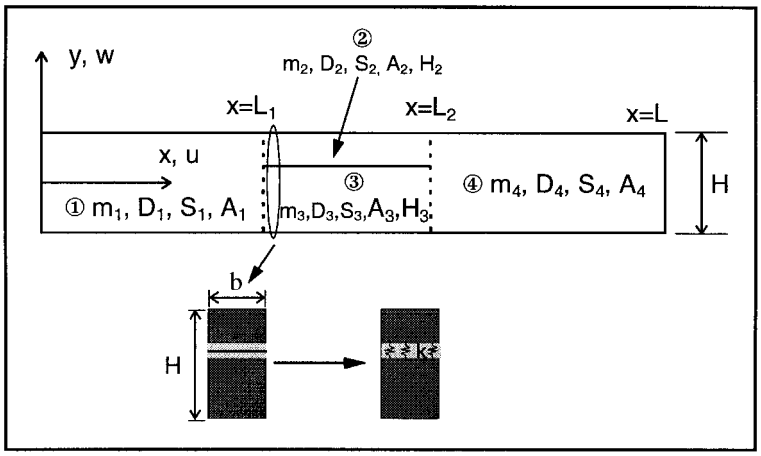

Fig. 1. Modeling of delamination effects.

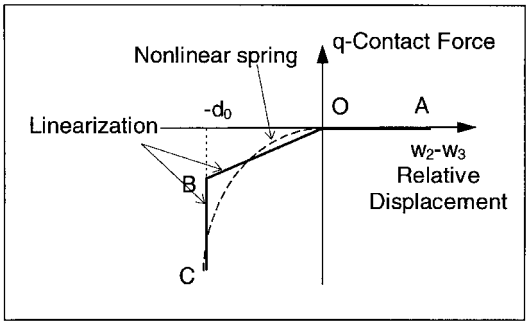

Fig. 2. A piecewise linear spring model.

delaminated beam, we reduced the nonlinear model into a piecewise linear model based on the following observations:

- When the delamination tends to open in vibrations, that is, the relative displacement $w_2 - w_3$ is positive, the distributed contact force is zero. The spring model is represented by the solid line OA in Fig. 2.
- When the delamination is completely closed during the vibrations, the relative displacement $w_2 - w_3$ is a fixed value. Under such a circumstance, the spring model can be simplified by another straight line BC as shown in Fig. 2.
- When the delamination beam is vibrating in a small amount of relative displacement, for example $-d_0 < w_2 - w_3 < 0$, the spring model can be simplified by a linear spring constant model, as shown in Fig. 2 by a solid straight line OB. For a given practical problem, the exact value for d_0 and spring constant in this region need to be determined by special experiments.

2.2. Equations of motion of delaminated structures

With the above considerations, the governing equations for free vibrations of a delaminated beam can be written as (under the sign convection for bending moment M and shear force V shown in Fig. 3):

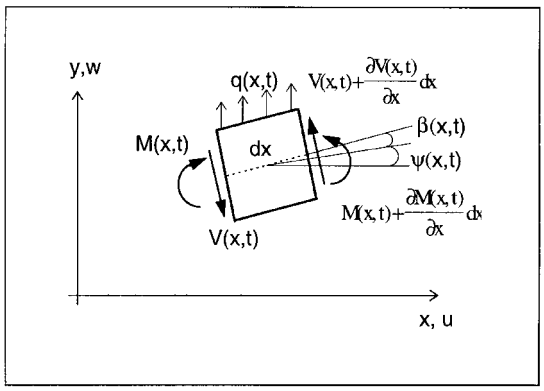

Fig. 3. Sign convention in bending.

$$A_i\frac{\partial^2 u_i}{\partial x^2} - m_i\frac{\partial^2 u_i}{\partial t^2} = P_i(x, t), \quad i = 1, 2, 3, 4 \tag{1}$$

for axial vibration, where i denotes the number of beam sections as shown in Fig. 1.

$$\frac{\partial}{\partial x}(S_i\beta_i) - m_i\frac{\partial^2 w_i}{\partial t^2} = F_{1i}(x, t)$$

$$\frac{\partial}{\partial x}\left(D_i\frac{\partial \psi_i}{\partial x}\right) + S_i\beta_i - J_i\frac{\partial^2 \psi_i}{\partial t^2} = F_{2i}(x, t); \quad i = 1, 4 \tag{2}$$

for flexural vibrations of intact beam segments, and

$$\frac{\partial}{\partial x}(S_i\beta_i) - m_i\frac{\partial^2 w_i}{\partial t^2} + q_i = F_{1i}(x, t)$$

$$\frac{\partial}{\partial x}\left(D_i\frac{\partial \psi_i}{\partial x}\right) + S_i\beta_i - J_i\frac{\partial^2 \psi_i}{\partial t^2} = F_{2i}(x, t); \quad i = 2, 3 \tag{3}$$

for flexural vibrations of delaminated sublaminates.

In these equations, u_i and w_i denote the axial and flexural displacements, respectively; β_i is the angle of the shear at the beam segment neutral axis; ψ_i is the slope of the deflection curve caused by bending moment; m_i is the mass per unit length; J_i is the cross sectional mass moment of inertia; q_i is distributed lateral load.

The w_i, β_i, and ψ_i are connected by

$$\frac{\partial w_i(x, t)}{\partial x} = \psi_i(x, t) + \beta_i(x, t). \tag{4}$$

While q_i, has the form

$$q_2(x, t) = k\big[w_3(x, t) - w_2(x, t)\big]$$

$$q_3(x, t) = k\big[w_2(x, t) - w_3(x, t)\big] \tag{5}$$

where k is the piecewise linear spring constant.

$P_i(x, t)$ is the external axial force, F_{1i} and F_{2i} are generalized external forces. The most general forms are:

$$F_{1i}(x, t) = Q_i(x, t) + \sum_k P_i(t)\delta(x - x_k)$$

$$F_{2i}(x, t) = N_i(x, t) + \sum_k M_i(t)\delta(x - x_k)$$

where $Q_i(x, t)$ is the external distributed force; $P_i(t)$ is the external concentrated force at the location $x = x_k$; $N_i(x, t)$ is the external distributed moment; $M_i(t)$ is the external concentrated moment at the location $x = x_k$. Since P_i, F_{1i}, and F_{2i} are independent of the system variables, in the following eigenproblem

solution procedures, these terms are set to zero. In the dynamic response calculations, there terms can be included and solved by a nonlinear modal analysis technique.

The mechanical properties of beam segments are formed by

$$A_i = b\sum_{k=1}^{n_i}\bar{Q}_{11}^k(z_k - z_{k-1}), \quad D_i = \frac{b}{3}\sum_{k=1}^{n_i}\bar{Q}_{11}^k\left(z_k^3 - z_{k-1}^3\right), \quad S_i = k'b\sum_{k=1}^{n_i}\bar{Q}_{55}^k(z_k - z_{k-1})$$

$$m_i = b\sum_{k=1}^{n_i}\rho^k(z_i - z_{k-1}), \quad J_i = \frac{b}{3}\sum_{k=1}^{n_i}\rho^k\left(z_k^3 - z_{k-1}^3\right)$$

where b is the width of the beam, ρ is the volume mass density of the lamina, z_k and z_{k-1} are the location of the k-th lamina with respect to the neutral axis of the i-th beam segment, n_i is the number of plies of the beam, k' is the shear correction factor, and $\bar{Q}_{11}^k$ and $\bar{Q}_{55}^k$ are stiffness coefficients of a lamina in the composite beam direction. The symbols $\bar{Q}_{11}^k$ and $\bar{Q}_{55}^k$ are further defined as

$$\bar{Q}_{11}^k = Q_{11}^k\cos^4\phi + Q_{22}^k\sin^4\phi + 2\left(Q_{11}^k + 2Q_{66}^k\right)\cos^2\phi\sin^2\phi$$

$$\bar{Q}_{55}^k = Q_{55}^k\cos^2\phi + Q_{44}^k\sin^2\phi$$

where ϕ is the angle of k-th lamina orientation with respect to the composite beam coordinates, and Q_{ij}^k are lamina stiffness coefficients in the ply coordinates.

Using eqn (4), eqn (2) are reduced to

$$\frac{\partial^4 w_1}{\partial x^4} - \left(\frac{m_1}{S_1} + \frac{J_1}{D_1}\right)\frac{\partial^4 w_1}{\partial x^2\,\partial t^2} + \frac{m_1}{D_1}\frac{\partial^2 w_1}{\partial t^2} + \frac{J_1 m_1}{D_1 S_1}\frac{\partial^4 w_1}{\partial t^4} = 0$$

$$\frac{\partial^4 w_4}{\partial x^4} - \left(\frac{m_1}{S_1} + \frac{J_1}{D_1}\right)\frac{\partial^4 w_4}{\partial x^2\,\partial t^2} + \frac{m_1}{D_1}\frac{\partial^2 w_4}{\partial t^2} + \frac{J_1 m_1}{D_1 S_1}\frac{\partial^4 w_4}{\partial t^4} = 0 \tag{6}$$

Similarly, by using eqn (4), eqns in (3) can be reduced to

$$\begin{aligned}&\frac{\partial^4 w_2}{\partial x^4}p - \left(\frac{m_2}{S_2} + \frac{J_2}{D_2}\right)\frac{\partial^4 w_2}{\partial x^2\,\partial t^2} + \frac{m_2}{D_2}\frac{\partial^2 w_2}{\partial t^2} + \frac{J_2 m_2}{D_2 S_2}\frac{\partial^4 w_4}{\partial t^4}\\ &\quad = \frac{k}{D_2}(w_3 - w_2) + \frac{J_2 k}{D_2 S_2}\left(\frac{\partial^2 w_3}{\partial t^2} - \frac{\partial^2 w_2}{\partial t^2}\right) - \frac{k}{S_2}\left(\frac{\partial^2 w_3}{\partial x^2} - \frac{\partial^2 w_2}{\partial x^2}\right)\end{aligned}$$

$$\begin{aligned}&\frac{\partial^4 w_3}{\partial x^4} - \left(\frac{m_3}{S_3} + \frac{J_3}{D_3}\right)\frac{\partial^4 w_3}{\partial x^2\,\partial t^2} + \frac{m_3}{D_3}\frac{\partial^2 w_3}{\partial t^2} + \frac{J_3 m_3}{D_3 S_3}\frac{\partial^4 w_3}{\partial t^4}\\ &\quad = \frac{k}{D_3}(w_2 - w_3) + \frac{J_3 k}{D_3 S_3}\left(\frac{\partial^2 w_2}{\partial t^2} - \frac{\partial^2 w_3}{\partial t^2}\right) - \frac{k}{S_3}\left(\frac{\partial^2 w_2}{\partial x^2} - \frac{\partial^2 w_3}{\partial x^2}\right)\end{aligned} \tag{7}$$

Note that the 'free model' of reference (Wang et al., 1982) corresponds to $k = 0$ case in eqn (7), while in the case where delamination is closed, $w_2 - w_3 = -d_0 =$ constant. By substituting $w_2 = w_3 - d_0$, eqns (7) can be further simplified as

$$\frac{\partial^4 w_3}{\partial x^4} - \left(\frac{m_2}{S_2} + \frac{J_2}{D_2}\right)\frac{\partial^4 w_3}{\partial x^2\,\partial t^2} + \frac{m_2}{D_2}\frac{\partial^2 w_3}{\partial t^2} + \frac{J_2 m_2}{D_2 S_2}\frac{\partial^4 w_3}{\partial t^4} = \frac{k}{D_2}d_0$$

$$\frac{\partial^4 w_3}{\partial x^4} - \left(\frac{m_3}{S_3} + \frac{J_3}{D_3}\right)\frac{\partial^4 w_3}{\partial x^2\,\partial t^2} + \frac{m_3}{D_3}\frac{\partial^2 w_3}{\partial t^2} + \frac{J_3 m_3}{D_3 S_3}\frac{\partial^4 w_3}{\partial t^4} = -\frac{k}{D_3}d_0 \tag{7a}$$

or

$$\begin{aligned}(D_2 + D_3)\frac{\partial^4 w_3}{\partial x^4} - \left(\frac{m_2 D_2}{S_2} + \frac{m_3 D_3}{S_3} + J_2 + J_3\right)\frac{\partial^4 w_3}{\partial x^2\,\partial t^2} \\ + (m_2 + m_3)\frac{\partial^2 w_3}{\partial t_2} + \left(\frac{J_2 m_2}{S_2} + \frac{J_3 m_3}{S_3}\right)\frac{\partial^4 w_3}{\partial t^4} = 0\end{aligned} \tag{7b}$$

It is seen that eqn (7b) is corresponding to the so-called 'constrained' model of reference (Mujumdar and Suryanarayan, 1988).

Assuming free harmonic vibration, i.e. let $u_i(x, t) = u_i(x)\mathrm{e}^{j\omega t}$, $w_i(x, t) = w_i(w)\mathrm{e}^{j\omega t}$, and nondimensionalizing x with $x = L\xi$, we get

$$\frac{\mathrm{d}^2 u_i}{\mathrm{d}\xi^2} + \gamma_i^2 u_i = 0, \quad i = 1, 2, 3, 4 \tag{8}$$

$$\frac{\mathrm{d}^4 w_i}{\mathrm{d}\xi^4} + 2b_1\frac{\mathrm{d}^2 w_i}{\mathrm{d}\xi^2} + c_1 w_i = 0, \quad i = 1, 4 \tag{9}$$

$$\frac{\mathrm{d}^4 w_2}{\mathrm{d}\xi^4} + 2b_2\frac{\mathrm{d}^2 w_2}{\mathrm{d}\xi^2} + c_2 w_2 = d_2(w_3 - w_2) + e_2\left(\frac{\mathrm{d}^2 w_3}{\mathrm{d}\xi^2} - \frac{\mathrm{d}^2 w_2}{\mathrm{d}\xi_2}\right) \tag{10}$$

$$\frac{\mathrm{d}^4 w_3}{\mathrm{d}\xi^4} + 2b_3\frac{\mathrm{d}^2 w_3}{\mathrm{d}\xi^2} + c_3 w_3 = d_3(w_2 - w_3) + e_3\left(\frac{\mathrm{d}^2 w_2}{\mathrm{d}\xi^2} - \frac{\mathrm{d}^2 w_3}{\mathrm{d}\xi_2}\right) \tag{11}$$

where

$$\gamma_i^2 = \frac{m_i\omega^2 L^2}{A_i}, \quad i = 1, 2, 3, 4$$

$$2b_i = \left(\frac{m_i}{S_i} + \frac{J_i}{D_i}\right)\omega^2 L^2, \quad c_i = \left(\frac{J_i\omega^2}{S_i} - 1\right)\frac{m_i}{D_i}\omega^2 L^4, \quad i = 1, 2, 3$$

$$d_i = \frac{kL^4}{D_i}\left(1 - \frac{J_i\omega^2}{S_i}\right), \quad e_i = -\frac{kL^2}{S_i}, \quad i = 2, 3$$

For beams with moderate to high slenderness ratio and low order of delamination opening modes, $-(e_i/d_i) \ll 1$, thus, it is reasonable to drop the second term in the right-hand-side of eqns (10) and (11). From eqn (10), we have

$$w_3 = \left(1 + \frac{c_2}{d_2}\right) w_2 + \frac{2b_2}{d_2}\frac{\mathrm{d}^2 w_2}{\mathrm{d}\xi^2} + \frac{1}{d_2}\frac{\mathrm{d}^4 w_2}{\mathrm{d}\xi^4} \tag{12}$$

Substituting (12) and (11) leads to

$$\frac{\mathrm{d}^8 w_2}{\mathrm{d}\xi^8} + \hat{a}_1\frac{\mathrm{d}^6 w_2}{\mathrm{d}\xi^6} + \hat{a}_2\frac{\mathrm{d}^4 w_2}{\mathrm{d}\xi^4} + \hat{a}_3\frac{\mathrm{d}^2 w_2}{\mathrm{d}\xi^2} + \hat{a}_4 w_2 = 0 \tag{13}$$

where

$$\hat{a}_1 = 2(b_2 + b_3), \quad \hat{a}_2 = c_2 + d_2 + c_3 + d_3 + 4b_2 b_3$$

$$\hat{a}_3 = 2\big[b_3(c_2 + d_3) + b_2(c_3 + d_3)\big], \quad \hat{a}_4 = c_2 c_3 + c_2 d_3 + c_3 d_2$$

For a cantilever beam clamped at $x = 0$ and free $x = L$, the axial deformation, using the boundary conditions of $u_1|_{\xi=0} = 0$, $\mathrm{d}u_1/\mathrm{d}\xi|_{\xi=1} = 0$, becomes

$$u_1 = C_1 \sin\left(\gamma_1 \xi\right)$$

$$u_2 = C_2 \sin\left(\gamma_2 \xi\right) + C_3 \cos\left(\gamma_2 \xi\right)$$

$$u_3 = C_4 \sin\left(\gamma_3 \xi\right) + C_5 \cos\left(\gamma_3 \xi\right)$$

$$u_4 = C_6 \cos\left[\gamma_1(\xi - 1)\right] \tag{14}$$

Solution forms for other boundary conditions can be obtained without any difficulty.

Based on eqn (9), we assume

$$w_1 = C_7 \sin\left(\alpha_1 \xi\right) + C_8 \cos\left(\alpha_1 \xi\right) + C_9 \sinh\left(\beta_1 \xi\right) + C_{10} \cosh\left(\beta_1 \xi\right)$$

$$w_4 = C_{11} \sin\left(\alpha_1 \xi\right) + C_{12} \cos\left(\alpha_1 \xi\right) + C_{13} \sinh\left(\beta_1 \xi\right) + C_{14} \cosh\left(\beta_1 \xi\right) \tag{15}$$

where

$$\alpha_1^2 = b_1 + \sqrt{b_1^2 - c_1}, \quad \beta_1^2 = -b_1 + \sqrt{b_1^2 - c_1}$$

It is easy to verify that the following expressions for ψ_1 and ψ_4 satisfy equations of motion:

$$\psi_1 = -C_7 \bar{\alpha}_1 \cos\left(\alpha_1 \xi\right) + C_8 \bar{\alpha}_1 \sin\left(\alpha_1 \xi\right) + C_9 \bar{\beta}_1 \cosh\left(\beta_1 \xi\right) + C_{10} \bar{\beta}_1 \sinh\left(\beta_1 \xi\right)$$

$$\psi_4 = -C_{11} \bar{\alpha}_1 \cos\left(\alpha_1 \xi\right) + C_{12} \bar{\alpha}_1 \sin\left(\alpha_1 \xi\right) + C_{13} \bar{\beta}_1 \cosh\left(\beta_1 \xi\right) + C_{14} \bar{\beta}_1 \sinh\left(\beta_1 \xi\right) \tag{16}$$

where

$$\bar{\alpha}_1 = \frac{\dfrac{m_1 \omega^2 L^2}{S_1} - \alpha_1^2}{\alpha_1 L}, \quad \bar{\beta}_1 = \frac{\dfrac{m_1 \omega^2 L^2}{S_1} - \beta_1^2}{\beta_1 L}.$$

In certain cases of small k/E_{av}, we can get real and pure imaginary roots from the characteristic equation of eqn (13). Under such circumstances, we assume solutions for eqns (13) and (12),

$$\begin{aligned} w_2 &= C_{15}\sin(\alpha_2\xi) + C_{16}\cos(\alpha_2\xi) + C_{17}\sin(\alpha_3\xi) + C_{18}\cos(\alpha_3\xi) \\ &\quad + C_{19}\sinh(\beta_2\xi) + C_{20}\cosh(\beta_2\xi) + C_{21}\sinh(\beta_3\xi) + C_{22}\cosh(\beta_3\xi) \\ w_3 &= C_{15}\hat{a}_2\sin(\alpha_2\xi) + C_{16}\hat{\alpha}_2\cos(\alpha_2\xi) + C_{17}\hat{\alpha}_3\sin(\alpha_3\xi) + C_{18}\hat{\alpha}_3\cos(\alpha_3\xi) \\ &\quad + C_{19}\hat{\beta}_2\sinh(\beta_2\xi) + C_{20}\hat{\beta}_2\cosh(\beta_2\xi) + C_{21}\hat{\beta}_3\sinh(\beta_3\xi) + C_{22}\hat{\beta}_3\cosh(\beta_3\xi) \end{aligned} \tag{17}$$

where α_2 and α_3 satisfy

$$x^4 - \hat{a}_1x^3 + \hat{a}_2x^2 - \hat{a}_3x + \hat{a}_4 = 0$$

while β_2 and β_3 satisfy

$$x^4 + \hat{a}_1x^3 + \hat{a}_2x^2 + \hat{a}_3x + \hat{a}_4 = 0$$

and

$$\hat{\alpha}_i = \frac{\left(c_2 + d_2 - 2b_2\alpha_i^2 + \alpha_i^4\right)}{d_2}, \quad \hat{\beta}_i = \frac{\left(c_2 + d_2 - 2b_2\beta_i^2 + \beta_i^4\right)}{d_2}, \quad i = 2, 3$$

Similarly, to satisfy eqn (3), we assume

$$\begin{aligned} \psi_2 &= -C_{15}\bar{\alpha}_2\cos(\alpha_2\xi) + C_{16}\bar{\alpha}_2\sin(\alpha_2\xi) - C_{17}\bar{\alpha}_3\cos(\alpha_3\xi) + C_{18}\bar{\alpha}_3\sin(\alpha_3\xi) \\ &\quad + C_9\bar{\beta}_2\cosh(\beta_2\xi) + C_{20}\bar{\beta}_2\sinh(\beta_2\xi) + C_{21}\bar{\beta}_3\cosh(\beta_3\xi) + C_{22}\bar{\beta}_3\sinh(\beta_3\xi) \\ \psi_3 &= -C_{15}\tilde{\alpha}_2\cos(\alpha_2\xi) + C_{16}\tilde{\alpha}_2\sin(\alpha_2\xi) - C_{17}\tilde{\alpha}_3\cos(\alpha_3\xi) + C_{18}\tilde{\alpha}_3\sin(\alpha_3\xi) \\ &\quad + C_{19}\tilde{\beta}_2\cosh(\beta_2\xi) + C_{20}\tilde{\beta}_2\sinh(\beta_2\xi) + C_{21}\tilde{\beta}_3\cosh(\beta_3\xi) + C_{22}\tilde{\beta}_3\sinh(\beta_3\xi) \end{aligned} \tag{18}$$

where

$$\bar{\alpha}_i = \frac{\frac{m_2\omega^2L^2}{S_2} - \alpha_i^2 + \frac{kL^2}{S_2}(\hat{\alpha}_i - 1)}{\alpha_iL}, \quad \bar{\beta}_i = \frac{\frac{m_2\omega^2L^2}{S_2} - \beta_i^2 + \frac{kL^2}{S_2}\left(\hat{\beta}_i - 1\right)}{\beta_iL}$$

$$\tilde{\alpha}_i = \frac{\frac{m_3\omega^2L^2}{S_3}\hat{\alpha}_i - \alpha_i^2\hat{\alpha}_i + \frac{kL^2}{S_3}(1 - \hat{\alpha}_i)}{\alpha_iL}, \quad \tilde{\beta}_i = \frac{\frac{m_3\omega^2L^2}{S_3}\hat{\beta}_i - \beta_i^2\hat{\beta}_i + \frac{kL^2}{S_3}\left(1 - \hat{\beta}_i\right)}{\beta_iL}, \quad i = 2, 3$$

Eqns (14)–(18) give general solution forms for a delaminated cantilever beam. Twenty two unknowns, $C_i (i = 1, 2, \ldots, 22)$, and the frequency parameter, ω, are determined by the following boundary conditions:

At $\xi = 0$ ($x = 0$):

$$w_1 = 0; \psi_1 = 0 \tag{19}$$

At $\xi = 1(x = L)$:

$$\psi_1' = 0, \quad w_4' - \psi_4 = 0 \tag{20}$$

At $\xi = \xi_1(x = L_1)$:

$$\begin{aligned} w_1 &= w_2, \quad w_1 = w_3, \quad \psi_1 = \psi_2, \quad \psi_1 = \psi_3 \\ u_2 &= u_1 - w_1' \frac{H_2}{L}, \quad u_3 = u_1 + w_1' \frac{H_3}{L} \\ D_1\psi_1' &= D_2\psi_2' + D_3\psi_3' - A_2u_2' + A_3u_3' \\ S_1(w_1' - \psi_1') &= S_2(w_2' - \psi_2') + S_3(w_3' - \psi_3') \\ A_1u_1' &= A_2u_2' + A_3u_3' \end{aligned} \tag{21}$$

At $\xi = \xi_2(x = L_2)$:

$$\begin{aligned} w_4 &= w_2, \quad w_4 = w_3, \quad \psi_4 = \psi_2, \quad \psi_4 = \psi_3 \\ u_2 &= u_4 - w_4' \frac{H_2}{L}, \quad u_3 = u_4 + w_4' \frac{H_3}{L} \\ D_4\psi_4' &= D_2\psi_2' + D_3\psi_3' - A_2u_2' + A_3u_3' \\ S_4(w_4' - \psi_4') &= S_2(w_2' - \psi_2') + S_3(w_3' - \psi_3') \\ A_4u_4' &= A_2u_2' + A_3u_3' \end{aligned} \tag{22}$$

Eqns (19)–(22) provide 22 homogeneous equations for 22 unknowns $C_i(i = 1, 2, \ldots, 22)$. The existence of nontrivial solution for C_i's requires the determinant of the coefficient matrix be zero, which forms the characteristic equation for solving eigenvalues. For each eigenvalue, the corresponding mode shape is determined by the eigenvector solution of the equations.

3. Examples

An example used were taken from reference by Shen and Grady (1992). Numerical predictions based on the proposed model were compared with the experimental results in the reference. Delamination opening modes were predicted by the proposed model. Using a nonlinear modal analysis technique and the proposed model, nonlinear free vibration response was predicted.

Table 1
Material properties of T300/934 graphite/epoxy prepreg

E_L	19.5 msi
E_T	1.5 msi
G_{LT}	0.725 msi
n_{LT}	0.33
ν_{TT}	0.60
ρ	1.3821e-4 lb-s^2/in^4

3.1. Specimen configuration

Material properties are listed in Table 1. In the reference, the transverse shear modulus is not given, even though in their finite element model shear effect was taken into consideration. The transverse shear modulus is usually hard to obtain. In our examples, we assume the composite lamina is transversely isotropic and the transverse Poisson ratio was selected as $\nu_{TT} = 0.6$, which is a reasonable guess according to reference (Zweben et al., 1989). Based on Table 1, the principal material stiffness coefficients are expressed as

$$\nu_{TL} = \frac{\nu_{LT} E_T}{E_L}, \quad G_{TT} = \frac{E_T}{2(1+\nu_{TT})}$$

$$Q_{11} = \frac{E_L}{1-\nu_{LT}\nu_{TL}}, \quad Q_{12} = \frac{\nu_{TL} E_L}{1-\nu_{LT}\nu_{TL}}, \quad Q_{22} = \frac{E_T}{1-\nu_{LT}\nu_{TL}}$$

$$Q_{44} = Q_{66} = G_{LT}, \quad Q_{55} = G_{TT}$$

Examples considered include cantilever composite beams with the eight-ply $[0/90]_{2s}$ construction and dimensions of $10 \times 0.5 \times 0.04'$. Thickness direction delamination locations are defined as in Shen and Grady (1992), i.e., 'Interface 1' implies the mid-plane delamination, while 'Interface 4' implies the skin ply delamination and so on. Lengthwise delamination locations are at the middle of beams. Delamination size includes 0 (intact), 1, 2, 3, and 4 inches.

Based on the model proposed and material properties given in the Table 1, a total of 17 cases including an intact beam and 16 delaminated beams with different delamination lengths and different delamination interfaces are calculated. Natural frequencies and mode shapes are compared with the experimental results provided in Shen and Grady (1992).

3.2. Natural frequencies

Based on the nonlinear model of this paper, for a delaminated beam, conceptually there is no 'natural frequency' as there is for intact beams. In the piecewise-linear model presented in the previous section, there are three distinct frequencies at different vibration amplitude levels. These frequencies correspond to the cases when $k \to \infty$, k equals a positive constant, and k equals 0. In Tables 2–5, we have shown the frequencies predicted by our model at $k = 0$, $k = 0.1$, $k \to \infty$ and the averaged frequencies measured in the experiments by Shen and Grady (1992). In Fig. 4, we have shown two extreme cases, $k = 0$ and $k \to \infty$, and experimental results for comparison.

From Tables 2–5 and Fig. 4, we can see that frequencies predicted by present model show reasonably good agreement with the experimental results, especially for the first three delamination interfaces. According to the present model, $k = 0$ and $k \to \infty$ predict the same frequency in cases where delaminations are small in length and not located on the neutral plane of the beam. In cases where the delamination length is large and the delamination thickness direction location is close to the beam surface, frequencies predicted by $k = 0$ and $k \to \infty$ are different. In Fig. 5, we have shown the delamination size and thickness location effects on first vibration frequencies, where DF is defined as the ratio of the frequency difference between $k = 0$ and $k \to \infty$ cases with respect to the intact case.

As expected, the significance of the intermediate k ($k = 0.1$ in the calculation) in the model is small if the delamination length is small and delamination is located close to the middle in the beam thickness direction (Tables 2 and 3). In these conditions, the delamination opening modes do not appear. As a result, the piecewise linear model yields to a 'constrained model'. However, as shown in Tables 4 and 5,

Table 2
Interface 1 frequencies (Hz)

Delamination	Intact	1 inch	2 inches	3 inches	4 inches
$k = 0$	81.859	81.452	76.807	67.641	56.953
$k = 0.1$	81.859	81.452	76.807	67.641	56.953
$k \to \infty$	81.859	81.452	76.807	67.641	56.953
Averaged test	79.833	78.167	75.369	67.959	57.542

Table 3
Interface 2 frequencies (Hz)

Delamination	Intact	1 inch	2 inches	3 inches	4 inches
$k = 0$	81.859	80.863	76.621	68.798	59.335
$k = 0.1$	81.859	80.863	76.621	68.798	59.335
$k \to \infty$	81.859	80.863	76.621	68.799	59.336
Averaged test	79.833	77.792	75.126	66.958	48.335

Table 4
Interface 3 frequencies (Hz)

Delamination	Intact	1 inch	2 inches	3 inches	4 inches
$k = 0$	81.859	82.009	80.740	77.520	71.727
$k = 0.1$	81.859	82.010	80.743	77.541	72.088
$k \to \infty$	81.859	82.015	80.785	77.823	73.148
Averaged test	79.833	80.125	79.750	76.958	72.460

Table 5
Interface 4 frequencies (Hz)

Delamination	Intact	1 inch	2 inches	3 inches	4 inches
$k = 0$	81.859	82.033	80.867	77.605	69.435
$k = 0.1$	81.859	82.034	80.892	77.719	69.928
$k \to \infty$	81.859	82.036	80.945	78.294	74.047
Averaged test	79.875	79.958	68.917	62.500	55.626

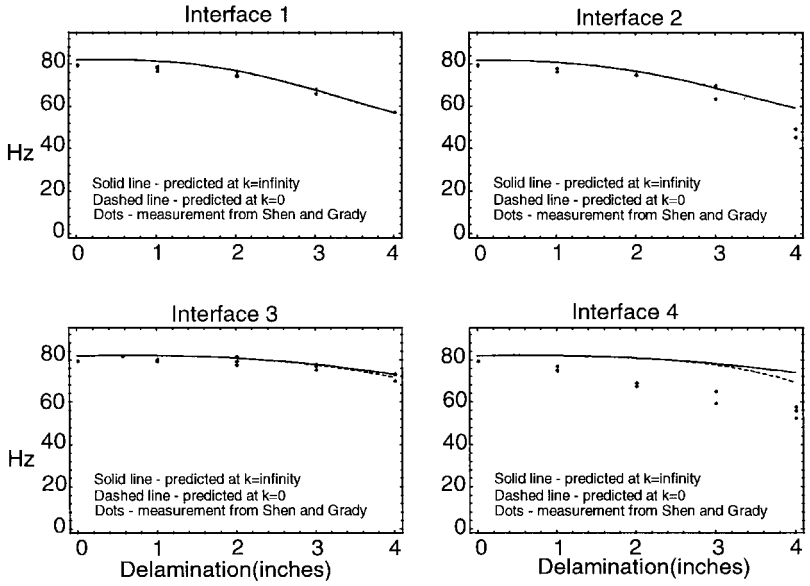

Fig. 4. Delaminated beam frequency predictions.

the significance of intermediate k becomes important if the delamination modes tend to appear. Different intermediate k yield different frequency which falls into the range bonded by the two frequencies obtained from extreme cases $k = 0$ and $k \to \infty$.

In Table 5 and Fig. 4, we see big discrepancies between experimental results and numerical results predicted by the present model for the delamination at Interface 4. This could be an experimental error. As shown in Fig. 6, the experimental results are even lower than the analytical prediction without considering the bending–stretching coupling effect, i.e., the bending stiffness in the delaminated region is simply the summation of the bending rigidities contributed by the delaminated sublaminates. It has been shown (Ramkumar et al., 1979; Wang et al., 1982) that without considering bending–stretching coupling, the analytical predictions should be consistently lower than the experimental results.

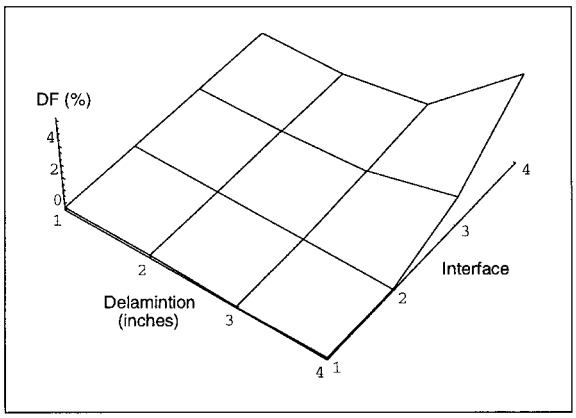

Fig. 5. Influence of the delamination size and location on the first vibration frequencies.

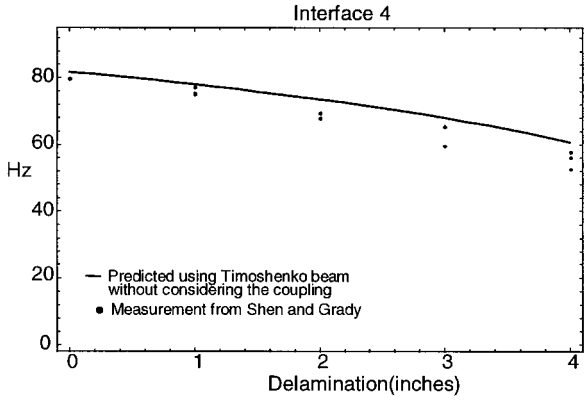

Fig. 6. Experimental measurements are lower than predictions without considering the bending–stretching coupling.

3.3. 'Mode shapes'

The present piecewise-linear model does not predict a unique mode shape as in a linear system, but the mode shape depend on the value of k which depends on the vibration amplitude. In Figs. 7–10, we have shown mode shapes of beams with different delamination location and size at $k = 0$.

From Figs. 7–10, we can see that first vibration modes do not show any opening in the cases of Interface 1 and 2 delaminations, while in cases of Interface 3 and 4 delaminations, we can clearly see the delamination opening modes except for the one inch delamination. By referring to Tables 2–5, it is clear that for modes where there is no opening in the delamination region, frequencies predicted by $k = 0$, $k \to \infty$, and $k = 0.1$ yield the same value or very close to each other. This is reasonable since if there is no opening in the delamination region, the 'free model' and 'constrained model' are essentially the same. However, in Shen and Grady (1992), results predicted by the Model A (corresponding to the 'constrained model') and the Model B (corresponding to the 'free model') are always different whether there is a delamination opening or not. Furthermore, for example, in the Interface 3 delamination cases,

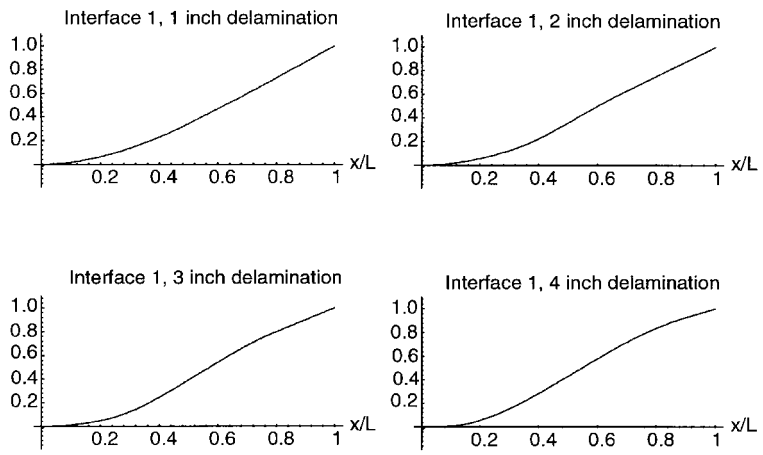

Fig. 7. Interface 1 mode shapes.

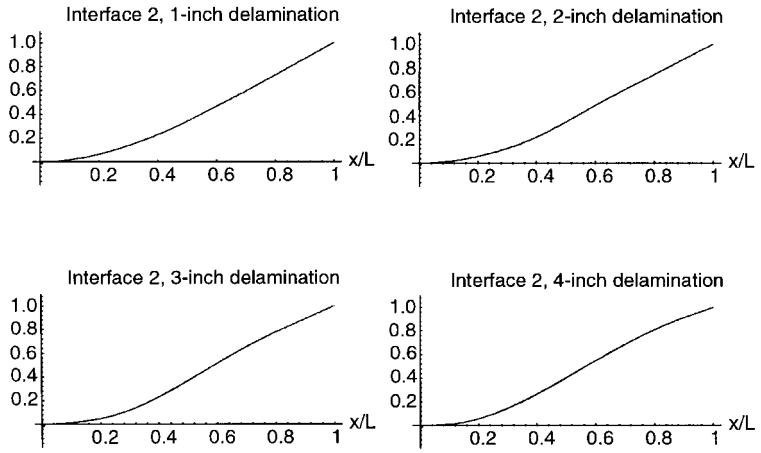

Fig. 8. Interface 2 mode shapes.

Model A, which is a 'constrained model', predicted a very close match with the test frequency data, while the experiments revealed clear delamination openings, especially for large lengths of delaminations.

3.4. Time response

For delaminated beam modes that display a delamination opening, a nonlinear response analysis becomes necessary to predict response correctly. A nonlinear modal analysis technique was employed for dynamic response calculations (Luo and Hanagud, 1997). In Fig. 11, we have shown the nonlinear free response of the beam with Interface 4, 4-inch delamination. In the calculations, we assume, as initial condition, that the beam is deformed in its first mode shape with $k \to \infty$ and then released. During free vibrations, we also assume mechanical energy in the beam can be transferred from one k value state to the other without losses, while energy transferred to higher modes is negligibly small. Since the first frequency at $k = 0$ is smaller than that at $k \to \infty$, under the same deformation, the potential energy stored in the $k = 0$ situation is smaller than that in the $k \to \infty$. Thus the positive vibration amplitude

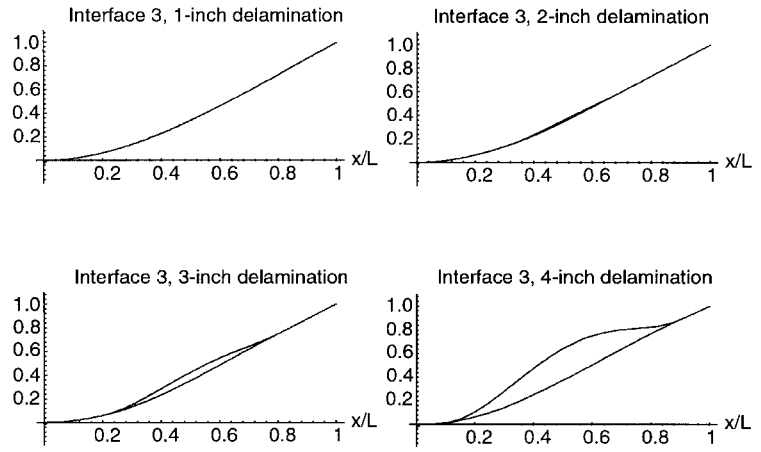

Fig. 9. Interface 3 mode shapes.

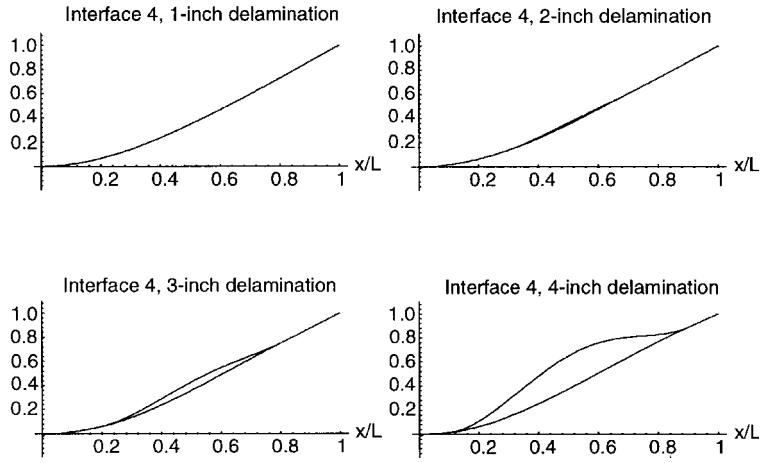

Fig. 10. Interface 4 mode shapes.

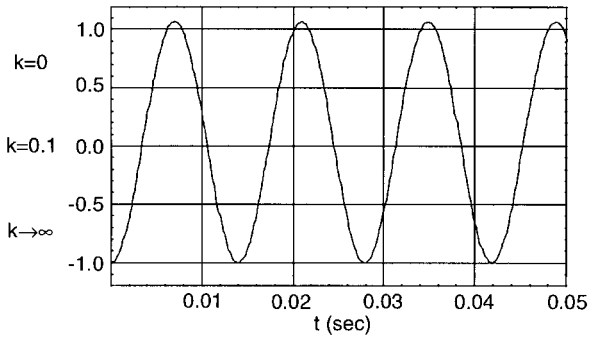

Fig. 11. Free response of delaminated beam at first frequency.

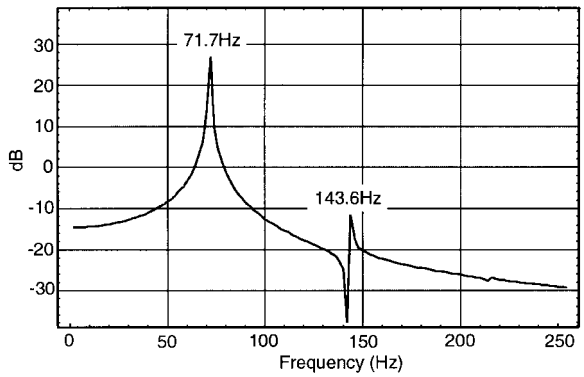

Fig. 12. The FFT analysis of the delamination response.

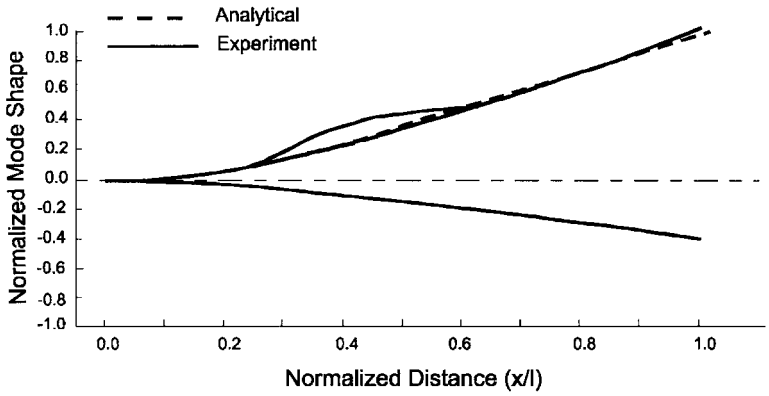

(a) Experimental Result Provided in Shen and Grady (1992)

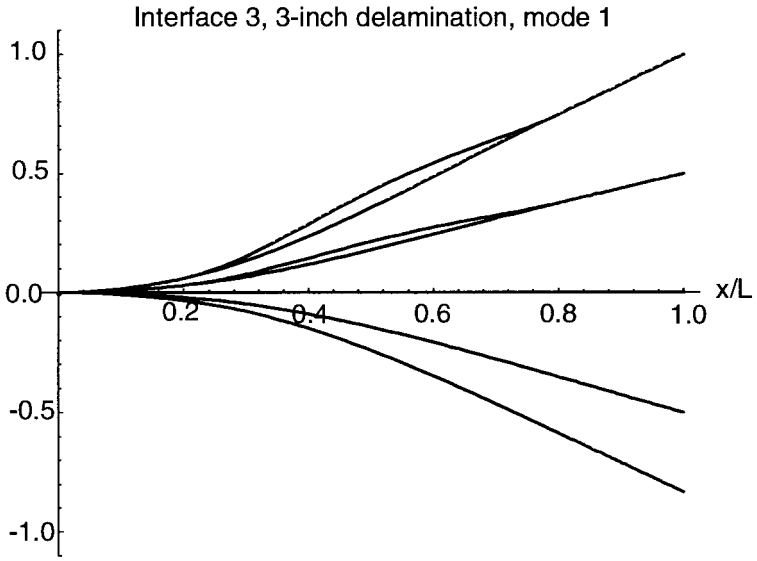

(b) Prediction Based on the Present Model

Fig. 13. Vibrations of the beam with Interface 3, 3-inch delamination. (a) Experimental result provided in Shen and Grady (1992); (b) prediction based on the present model.

calculated (see Fig. 11) is larger than the negative vibration amplitude, as expected. The Fast Fourier Transform analysis (FFT) has also indicated the nonlinearity in the response. In Fig. 12, we have shown the FFT analysis magnitude. The main peak is neither at the $k = 0$ resonance nor at the $k \to \infty$ resonance, but at somewhere in between. The existence of multiple peaks clearly indicates the superharmonic phenomena, which is a typical nonlinear effect.

By using the model presented in this paper, we are able to capture the experimentally revealed

delamination openings. For example, in Interface 3, 3-inch delamination case given in the reference by Shen and Grady (1992), it was shown that the frequency prediction based on model A had a very close match with the experimental data. Since model A was actually a 'constrained model', delamination openings could not be predicted. Fig. 13(a) is a comparison of the analytical and experimental results provided in reference by Shen and Grady (1992). In Fig. 13(b), we have shown the nonlinear response prediction based on the present model. It is clearly seen that a cycle of vibration includes delamination opening and closing.

4. Conclusions

In this paper, an analytical model for composite beams with through-width delaminations is presented. The model includes the rotary inertia and transverse shear effects as well as bending-extension effect in analysis. The effects between delaminated sublaminates are simplified as a piecewise-linear model. Previously proposed 'free model' and 'constrained model' are unified in the present model in two aspects:

1. When the delamination length is small and is located close to the geometric mid-plane, there is no significant delamination opening in the first mode and the nonlinear model approaches a linear model. Both 'free model' and 'constrained model' predict the same or nearly the same frequencies.
2. When the delamination is large and close to the beam surface, a delamination opening exists in vibrations. Nonlinear effects must be taken into consideration. A cycle of vibration response is a combination of the vibrations from both the 'free model' and the 'constrained model'.

Based on the piecewise-linear model, predicted frequencies show good agreement with experimental measurements. Mode shape predictions also reflect the experimental phenomena. Based on a nonlinear modal analysis technique, the proposed model is able to predict the nonlinear dynamic response.

This model provides a better understanding of a delaminated beam, which will, in turn, help to develop new delamination detection schemes based on structural dynamic response.

References

Anon, 1992. Inspect of composite structures. Aerospace Engineering, Warrendale, Pennsylvania 12 (5), 9–13.

Chen, H.-P., 1994. Free vibration of prebuckled and postbuckled plate with delamination. Composite Science and Technology 51, 451–462.

Garg, A.C., 1988. Delamination—a damage mode in composite structures. Engineering Fracture Mechanics 29, 557–584.

Hanagud, S., Luo, H., 1994. Modal analysis of a delaminated beam. In: Proceedings of SEM Spring Conference on Experimental Mechanics, 880–887.

Hwu, C., Hu, J.S., 1993. Flexural vibration of delaminated composite sandwich beams. In: Chandra, T., Dhingra, A.K. (Eds.), Advanced Composite '93, International Conference on Advanced Composite Materials. The Minerals and Materials Society, pp. 367–371.

Luo, H., Hanagud, S., 1995. Delamination detection using dynamic characteristics of composite plates. Proceedings of 36th AIAA/ASME/ASCE/AHS SDM Conference, 129–139.

Luo, H., Hanagud, S., 1997. Delaminated beam nonlinear dynamic response calculation and visualization. Proceedings of 38th AIAA/ASME/ASCE/AHS SDM Conference 1, 490–499.

Mujumdar, P.M., Suryanarayan, S., 1988. Flexural vibrations of beams with delaminations. Journal of Sound and Vibrations 125 (3), 441–461.

Nagesh Babu, G.L., Hanagud, S., 1990. Delamination in smart structures—a parametric study on vibrations. 31st SDM Conference, 2417–2426.

Ramkumar, R.L., Kulkarni, S.V., Pipes, R.B., 1979. Free vibration frequencies of a delaminated beam. 34th Annual Technical Conference, 1979 Reinforced Plastics/Composites Institute. The Society of the Plastics Industry Inc. 22-E, 1–5.

Shen, M.-H.H., Grady, J.E., 1992. Free vibrations of delaminated beams. AIAA Journal 30 (5), 1361–1370.
Tracy, J.J., Pardoen, G.C., 1989. Effect of delamination on the natural frequencies of composite laminates. Journal of Composite Materials 23, 1200–1215.
Wang, J.T.S., Liu, Y.Y., Gibby, J.A., 1982. Vibration of split beams. Journal of Sound and Vibrations 84 (4), 491–502.
Yin, W.L., Jane, K.C., 1992. Vibration of a delaminated beam-plate relative to buckled states. Journal of Sound and Vibration 156 (1), 125–140.
Zweben, C., Hahn, H.T., Chou, T.-W. (Eds.), 1989. Delaware Composite Design Encyclopedia—Volume 1, Mechanical Behavior and Properties of Composite Materials. Technomic Publishing Co. Inc.